

This is an Open Access document downloaded from ORCA, Cardiff University's institutional repository: <https://orca.cardiff.ac.uk/id/eprint/112196/>

This is the author's version of a work that was submitted to / accepted for publication.

Citation for final published version:

Schotten, Christiane, Howard, Joseph L., Jenkins, Robert L., Codina, Anna and Browne, Duncan L. 2018. A continuous flow-batch hybrid reactor for commodity chemical synthesis enabled by inline NMR and temperature monitoring. *Tetrahedron* 74 (38) , pp. 5503-5509. 10.1016/j.tet.2018.05.070

Publishers page: <http://dx.doi.org/10.1016/j.tet.2018.05.070>

Please note:

Changes made as a result of publishing processes such as copy-editing, formatting and page numbers may not be reflected in this version. For the definitive version of this publication, please refer to the published source. You are advised to consult the publisher's version if you wish to cite this paper.

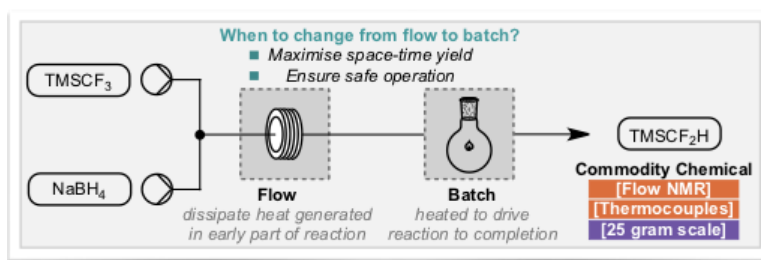
This version is being made available in accordance with publisher policies. See <http://orca.cf.ac.uk/policies.html> for usage policies. Copyright and moral rights for publications made available in ORCA are retained by the copyright holders.



A continuous flow-batch hybrid reactor for commodity chemical synthesis enabled by inline NMR and temperature monitoring

Christiane Schotten^a, Joseph L. Howard^a, Robert L. Jenkins^a, Anna Codina^b and Duncan L. Browne^{a*}

^a*School of Chemistry, Cardiff University, Park Place, Cardiff, CF10 3AT, UK* ^b*Bruker UK Limited, Banner Lane, Coventry, CV4 9GH, UK*



A continuous flow-batch hybrid reactor for commodity chemical synthesis enabled by inline NMR and temperature monitoring

Christiane Schotten^a, Joseph L. Howard^a, Robert L. Jenkins^a, Anna Codina^b and Duncan L. Browne^{a*}

^aSchool of Chemistry, Cardiff University, Park Place, Cardiff, CF10 3AT, UK

^bBruker UK Limited, Banner Lane, Coventry, CV4 9GH, UK

ARTICLE INFO

Article history:

Received

Received in revised form

Accepted

Available online

ABSTRACT

Inline, real time NMR and temperature measurements have been used to optimise the continuous flow synthesis of difluoromethyltrimethylsilane (TMSCF₂H) by the reduction of the Ruppert-Prakash reagent (TMSCF₃). These measurements were used to maximise the space-time-yield, while ensuring this exothermic process remains safe. In this way, a three-fold increase in space-time-yield was achieved compared to the reported batch procedure, isolating 25 g of pure TMSCF₂H after 105 minutes.

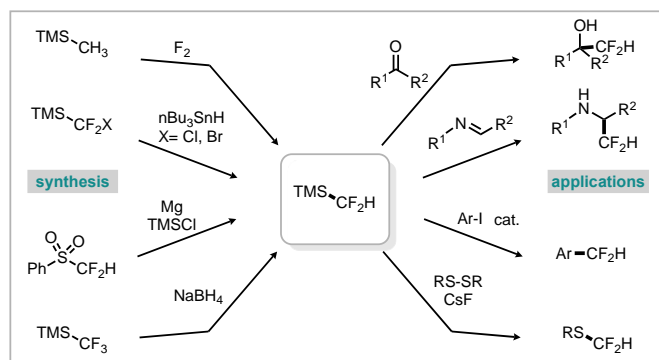
Keyword Continuous Flow, Flow NMR, Inline monitoring, exotherm control, Space Time Yield

1. Introduction

The synthesis of newly reported key reagents, reactants and building block intermediates is of great importance for expediting the discovery of molecules with improved properties. This is especially true for small molecules, where the fine-tuning of properties is typically achieved by late-stage reactions. Indeed, there is an increase in the number of reagents and methods reported for late-stage functionalisation reactions.¹ Implementation of such an approach at a research and development scale results in a high demand for the newly developed and reported reagents. Thus, there exists a requirement for commercial chemical suppliers to have reliable and safe access to new commodity chemicals in the forms of reagents and reactants.

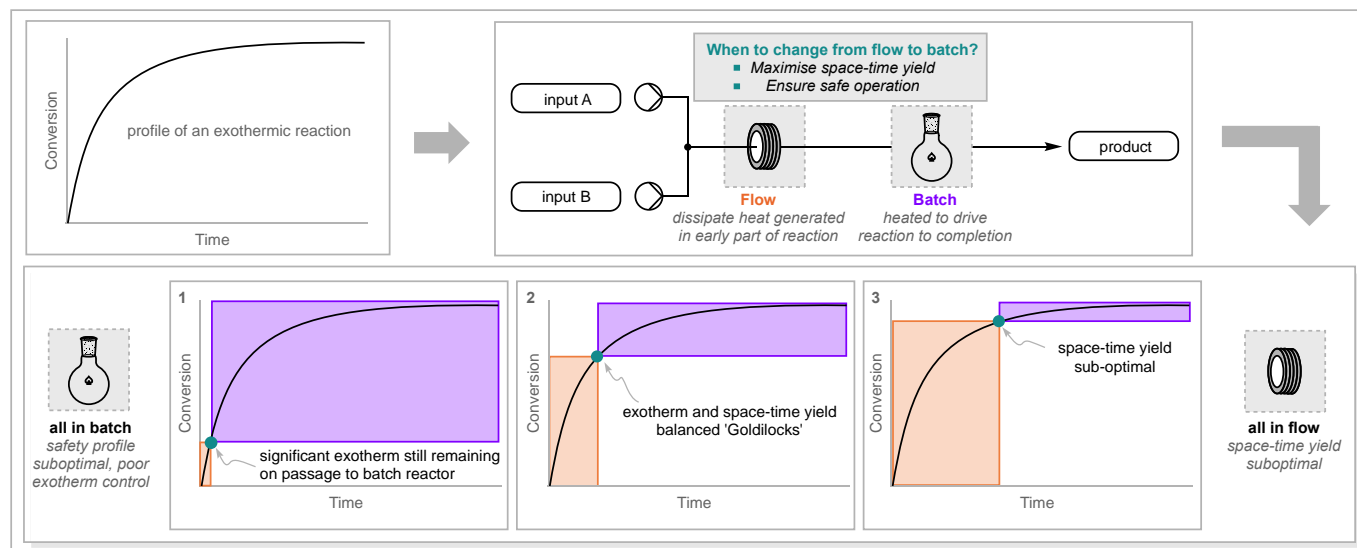
Recently, we have been interested in one such reagent; difluoromethyltrimethylsilane (TMSCF₂H). This material is capable of providing a nucleophilic source for difluoromethylation and has been applied to the treatment of imines, ketones and in metal catalysed processes (Scheme 1).² Our lab and others have reported the formation of difluoromethylthioethers through the treatment of disulfides with TMSCF₂H in the presence of a fluoride source.³ As part of this reaction development, several methods for the preparation of TMSCF₂H were explored; we found the reduction of the Ruppert-Prakash reagent (TMSCF₃) using sodium borohydride, as reported by Tyutyunov and co-workers, to be the most direct.⁴ Particularly notable about this process is the high reaction

exotherm (as well as some curious and unusual reactivity!) which, depending on solvent may be accompanied by a vigorous exotherm and even explosion.⁴ Indeed, we found that reaction in diglyme could not reliably be scaled beyond 10 g batches. Calling upon our previous experience in continuous flow processing and controlling of reactions that require low temperatures, we opted to explore the facile scale up of this exothermic reaction. It was ultimately planned to deliver a hybrid flow-batch route to this commodity chemical (Scheme 2). The flow component of the hybrid design would allow the bulk of the exotherm, generated in the early part of the reaction, to be better dissipated through the increased surface area to volume ratio.⁵ The flowing stream would then drop into the batch component,



Scheme 1 Synthesis and use of TMSCF₂H

* Corresponding author. Tel.: +44 (0)29 2087 5571; e-mail: dlbrowne@cardiff.ac.uk



Scheme 2 Deciding where to change from flow to batch to maximise efficiency and maintain safety

where the final part of the reaction could be completed under high temperature conditions whilst simultaneously distilling the product from this reaction pot. In so designing such a hybrid reactor, we considered where to make the change from flow to batch, **Scheme 2** shows three possible theoretical scenarios. Scenario 1) describes a situation where the exotherm is not fully dissipated before passing into the heated batch reactor and thus represents a potential safety risk, whereas scenario 3) represents a reactor where the space-time yield is suboptimal as the exotherm is essentially all dissipated and the reaction progression is now slow in the flow part of the reactor. Scenario 2) represents a 'Goldilocks' situation where the balance between safety and space-time- yield are in the optimal region. This analysis shows that such a hybrid design is actually thus prone to individual operator's targets and regulations for safety and space-time-yield.^{4b}

Continuous flow processing provides several advantages at scale compared to analogous reactions in batch mode operation. Owing to this, such methods are becoming widely used and explored for synthesis in both academia and industry.⁶ Recently, the ability to monitor reaction processes continuously has been further developed, particularly with regard to the equipment available for incorporation in to synthesis setups. Inline monitoring of a reaction provides the operator with significantly more understanding of a process than analysis after downstream processing, such as workup or solvent removal. Many standard analytical techniques have been adapted to provide inline, *in-situ* analysis in real time. These include IR, UV and NMR spectroscopy as well as mass spectrometry and HPLC.⁷ These methods have been used to simply ensure that a system is running correctly but also to measure yields and feedback to a computer control unit for automatic optimisation of reactions.^{7b, 7c, 8} Inline NMR spectroscopy is perhaps one of the most powerful tools as it can provide more structural information than the other techniques and is most familiar to the common day practice of a synthetic chemist. Indeed, the development of benchtop spectrometers, specially designed flow NMR probes and the necessary software has permitted inline NMR to become an accessible and useful technique.⁹

In this study, we describe the use of inline ¹⁹F NMR, in combination with temperature measurements, to optimise the preparation of the difluoromethylating reagent TMSCF₂H. In our setup, the Bruker InsightMR flow tube was used.¹⁰ This has

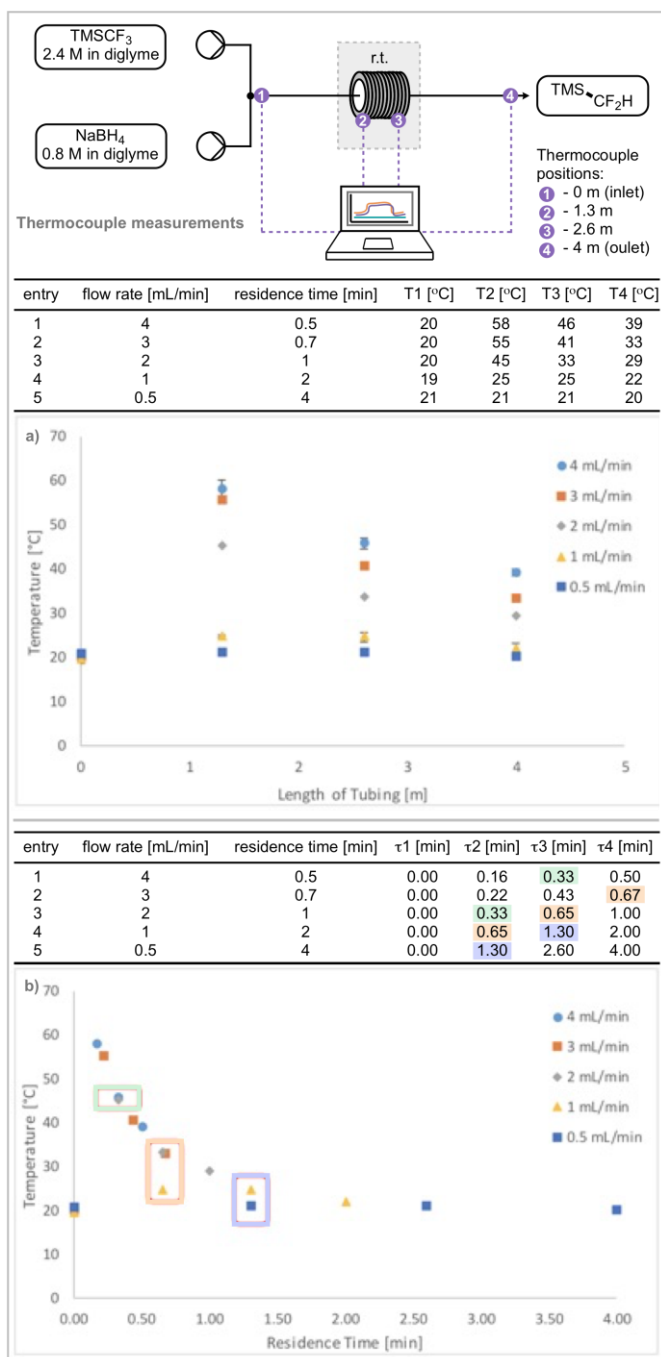
several desirable features, of which, perhaps the most important is that it can be used in high-field spectrometers by simply inserting it in the place of a normal NMR sample tube. This means that a range of multinuclear experiments are possible with high resolution and good sensitivity. This enables data to be acquired with few scans, so high quality spectra can be obtained frequently, giving good temporal resolution. The InsightMR tube is also designed to permit accurate control of temperature by incorporation of a recirculating chiller. For reactions monitored by ¹H NMR spectroscopy, the reaction in question needs to be run either with solvent suppression pulse sequences or in costly deuterated solvents. Whilst the equipment used in the present study is capable of solvent suppression simply by clicking the appropriate solvent from the software menu (pre-programmed sequencing), our particular reaction example was instead better suited to ¹⁹F NMR monitoring. By using ¹⁹F NMR, it was not necessary to use deuterated solvents or solvent suppression pulse sequences to acquire high quality spectra on the crude reaction mixture.

Inline, real time monitoring by multiple techniques can provide complementary information to optimise reaction conditions or ensure the system is stable. In combination with inline NMR analysis, we used a number of inexpensive thermocouples to measure the temperature at different points along the reactor coil. These thermocouples could be directly connected to a laptop and the data processed in real time using Microsoft Excel (See Supporting information for further details). It was envisaged that this temperature profile combined with information on the yield of the reaction from inline NMR data would allow optimisation of the space-time-yield for the synthesis of TMSCF₂H by choosing the most appropriate point to change from flow to batch.

2. Results and Discussion

2.1. Inline temperature measurements

The reduction of TMSCF₃ was performed in flow and initial results showed that temperature differences could be detected outside of the tubing. The commercially available thermocouple sensors were simply attached to the outside of the 4 m (2 mL) reactor coil (see Supporting Information for pictures and detailed measurement description).



Scheme 3 Results of inline temperature measurements a) Temperature change along the length of the reactor tube. b) Temperature change with respect to residence time.

The temperature at different points along the tube (T1: inlet, T2: 1/3 of the length, T3: 2/3 of the length, T4: outlet) was measured for different flow rates at steady state. It was expected that the temperature would initially increase when the rate of heat production exceeds the rate of dissipation. After the reaction had progressed sufficiently, it was expected that a peak temperature would be reached, after which the rate of dissipation exceeds the rate of heat production and the temperature would then decrease. After this point, the exotherm is deemed as being safely controlled and a thermal runaway is unlikely. By using four thermocouple sensors, the exact position and value of the temperature peak could not be determined, but it could be confirmed if the exotherm had been safely dissipated by the end of the reactor coil.

At all flow rates tested the temperature went through a maximum between T1 and T3, with the highest measured temperature at T2, and then decreased over the length of the tubing (**Scheme 3a**). At slow flow rates (0.5 mL/min and 1 mL/min), a negligible temperature change was detected, suggesting the exotherm was completely dissipated early in the reactor coil. The highest temperature was observed for the fastest flow rate (58 °C, T2 at 4 mL/min). For all flow rates, the temperature then decreased along the length of the reactor demonstrating that the exotherm was successfully dissipated. However, for the faster flow rates, the temperature at the outlet (T4) remained slightly above room temperature (**Scheme 3a**).

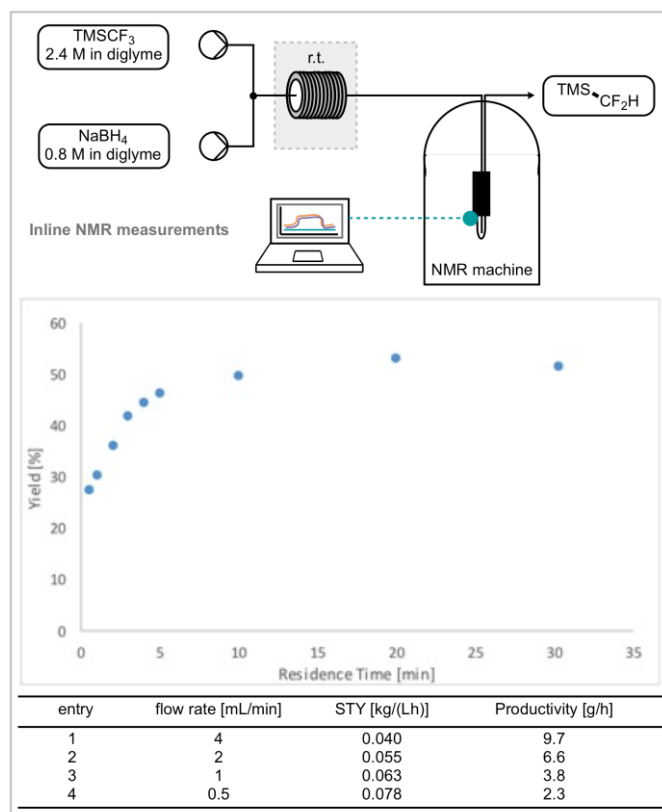
The temperature profile was also analysed with respect to the residence time (**Scheme 3b**) instead of the length of tubing. In general, this was as expected for an exothermic reaction. However, there are some points where for identical residence times but different flow rates different temperatures were observed. For these points, the faster flow rates exhibited higher temperatures despite having passed through a longer length of reactor coil. This suggests that the faster flow rates are accelerating the reaction, possibly through different mixing behaviour.

Having now established that the exotherm was dissipated at all flow rates tested, our attention was turned to measuring the performance of the reaction at different flow rates using inline NMR methods.

2.2. Inline NMR measurements

The reaction setup was modified to allow the quantitative analysis of our reaction by inline NMR. The reactor coil was directly attached to the Bruker InsightMR flow tube in order to allow direct yield determination at the reactor outlet (see Supporting Information for pictures and details of modification and measurements).

The yield of the reaction was determined using ^{19}F NMR with trifluorotoluene as internal standard. A number of considerations were required to achieve this. Firstly, the flow rates that could be used were limited by the NMR experiment to 4 mL/min. If the flow rate was too high, the nuclei excited by the radiofrequency pulse had already left the sample tube when the spectrometer recorded the fid. Secondly, in order to obtain reliable data on the composition at the reactor output, the measurements had to be taken at steady state, taking into account the additional volume of the sample chamber (approximately 1.6 mL). Finally, in order to achieve conditions in the reactor coil that were comparable to the temperature measurements, the Bruker InsightMR flow tube was modified to have the same dimensions as our reactor coil (see Supporting Information for further details). Using a high field spectrometer (500 MHz) allowed a single scan to be used to obtain quantitative data, so real time data on the composition of the reaction mixture could be obtained approximately every 5 seconds. The yield was measured for different flow rates at steady state according to the setup in **Scheme 4**. As expected, the yield increases with the residence time with a plateau of about 50% after 10 min (**Scheme 4**). However, even at short residence times (0.5 min) a yield of 27% is still observed (entry 9). It is noteworthy that the reaction still continued in the collection flask for the low yield entries.



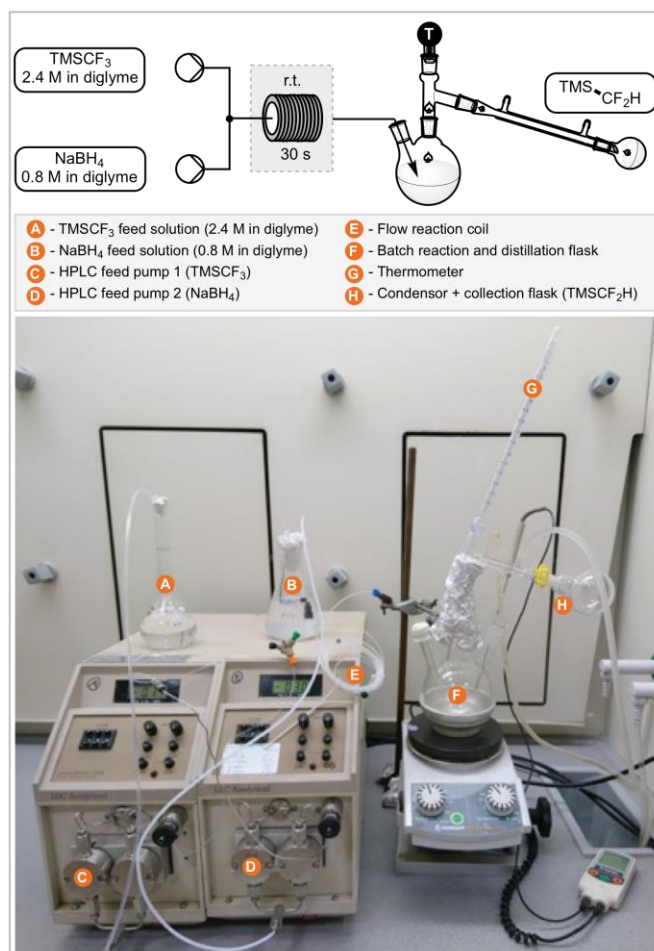
Scheme 4 Results of inline NMR measurements

2.3. Scale Up

With the information about the temperature profile and yields of the reaction in hand, it was now possible to design a setup that would allow safe, efficient production on a larger scale. As shown in **Scheme 2**, the optimal point at which to change from flow to batch could now be assessed. The space-time-yield (STY) and productivity were calculated using the information obtained from the inline NMR measurements. The space-time-yields are slightly higher for slow flow rates due to the higher yields. However, the productivity was greatest for the highest flow rate even for the non-completed reactions (**Scheme 4**). As the reaction is to be completed in batch, it is preferable to choose a high flow rate with the highest productivity. Initial studies (performed cautiously on small scales) demonstrated that although the outlet temperature for the faster flow rates remained above room temperature, when fed into a batch flask at 50 °C no thermal runaway occurred. Therefore, we decided to use the fastest flow rate for the scale up setup where the reaction would then be completed in batch and directly purified by distillation.

The flow output was collected directly into a distillation flask, allowing the reaction to be driven to completion by heating and to be distilled directly. This semi-continuous process has the potential for design improvements to achieve a continuous process, in which the flow reactor outlet has the potential to be directed to multiple distillation flasks using a multi-port single-input switching valve. These flasks can then be automatically emptied after distillation is complete and would then be ready to be filled again.

The outlet of the flow setup was fed into a two-necked flask equipped with a thermometer and condenser (**Scheme 5**). During the collection, the reaction was stirred at 50 °C. After determined collection volume had been reached stirring the reaction solution



Scheme 5 Setup for scaling up the reaction

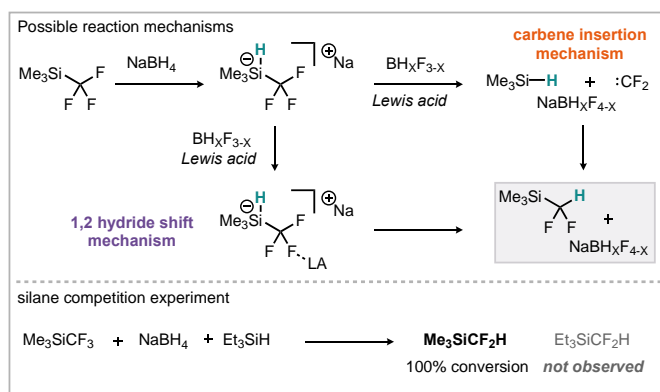
for an additional 30 min in the collection flask at 50 °C was required prior to distillation in order to ensure only TMSCF₂H was obtained (in the absence of this additional 30 minute stirring, TMSCF₃ could be found in the distillate).

Using this setup, 50 g of starting material was processed in a total of 105 min. After the additional 30 min of stirring, distillation yielded TMSCF₂H with traces of solvent which were removed by a second distillation to obtain pure product (25 g, 56%) with a STY of 0.048 kgL⁻¹h⁻¹.

These results allowed us to compare the space-time-yield of our telescoped process to the batch process. Typical procedures such as the one performed by Goossen and co-workers usually processed a maximum of 20 g of TMSCF₃ to yield 12 g TMSCF₂H (71% yield) in 12 h in batch giving a STY of 0.016 kgL⁻¹h⁻¹.²ⁿ

The hybrid flow-batch process developed here is therefore not only safer and easier to scale up, it also shows a threefold STY compared to the previously reported batch process mainly due to a significant decrease in time from 12 h to under 2 h.

Finally we were intrigued by the reaction mechanism of this exothermic process. We hypothesized two possible reaction pathways (**Scheme 6**), both of which commence with the formation of a silicate complex by hydride transfer from sodium borohydride onto the Ruppert-Prakash reagent. The fate of this silicate complex is then postulated to proceed via either a 1,2 hydride shift mechanism with concomitant loss of fluoride that could be facilitated by a borane (or related) Lewis acid species or a carbene mechanism. The latter process would instead involve



Scheme 6 Possible reaction mechanisms

the degradation of the silicate to trimethylsilane, difluorocarbene and boronate species, again facilitated by a boron derived Lewis acid, followed by insertion of the carbene into the Si-H bond to furnish the product. Analysis of this process by inline ¹⁹F NMR did not permit an understanding of this process in our hands. However, a silane competition experiment was designed to probe this reaction further. Addition of triethylsilane to the reaction mixture would compete with the putative trimethylsilane for the insertion of difluorocarbene and thus give rise to Et₃SiCF₂H. In the event, no Et₃SiCF₂H was observed thus favouring a hydride shift mechanism, although carbene generation inside a local stabilised solvent cage cannot be ruled out.

3. Conclusion

A continuous flow process for the monitoring and control of an exothermic reaction, the reduction of TMSCF₃ to TMSCF₂H, has been established. The temperature profile along the reactor was monitored *via* commercially available thermocouples and the yield determined by inline ¹⁹F NMR measurements using a high field spectrometer. This enabled the identification of a safe reaction regime and allowed scale up of the process in a telescoped semi-continuous approach. 50 g of starting material were processed in 105 min total reaction time to yield 25 g (56%) of clean material after distillation. Compared to the batch process a threefold improvement in space-time-yield was achieved.

4. Experimental section

4.1. General Methods

Trifluoromethyl trimethyl silane (TMSCF₃) and diethylene glycol dimethyl ether (diglyme) were purchased from Fluorochem (007685 and 075235). Sodium borohydride was purchased from Acros Organics (44850). TMSCF₃ and sodium borohydride were used without further purification. Diglyme was dried over CaH₂ and distilled prior to use. NMR measurements were conducted on a Bruker Avance III HD 500 MHz spectrometer equipped with a Prodigy Cryoprobe, using the InsightMR software (version 1.0.b22). The flow setup consisted of a modified version of InsightMR (see S3 in Supporting Information). The flow setup consisted of perfluoroalkoxy (PFA) tubing of an 0.8 mm ID, 1.2 mm OD supplied by Polyflon and two pumps. The residence coil was made from the tubing by taking the appropriate length (4 m) for the desired volume (2 mL). Fittings were supplied by Kinesis and part numbers given where appropriate. The thermocouples are xlogger (itec) parts with a temperature sensor, a reading panel and a USB adapter. In all cases solutions of the

two reactants were prepared separately before pumping them into the flow system where they were combined at a T-piece and passed through the reactor coil.

4.2. Inline temperature measurements

The temperature measurements were conducted using xlogger temperature sensors (itec) with the software being built-in to excel *via* a plug-in. The setup consists of a thermistor, temperature reading and a USB cable (See Supporting Information for full details). The sensors of each thermocouple were attached to the surface of the flow tubing with a cable tie at the inlet (about 1 cm), 1.3 m (1/3 of the length), 2.6 m (2/3 of the length) and at the outlet (4 m). They were insulated with cotton wool. Prior to use, the room temperature reading was taken for calibration. The room was thermostatically controlled, and the temperature was 19 °C during all measurements. The room temperature value of the thermocouples was corrected to that value. Solutions of TMSCF₃ (2.4 M in diglyme) and of sodium borohydride (0.8 M in diglyme) were pumped through the setup equipped with the thermocouples using syringe pumps. The temperature measurement was started when the flow was started. The temperature reading was taken after 8 residence times to ensure steady state. For 4 mL/min and 1 mL/min the measurement was repeated three times, the average taken and the standard error in the mean calculated to be a maximum of 2 °C.

4.3. Inline NMR measurements

The setup was modified to measure yields at different flow rates and residence times acquiring ¹⁹F NMR spectra using the Bruker InsightMR software (See Supporting Information). The flow tube was inserted into the NMR machine and the system flushed with a solution of trifluorotoluene (1.6 M) in diglyme. After stopping the pumps, the spectrometer was set to optimise the shim settings in respect to the ¹H spectrum of the solution and then tune back to ¹⁹F. After that the reaction measurements were started by pumping a solution of TMSCF₃ (2.4 M) and trifluorotoluene (1.6 M) in diglyme and a solution of sodium borohydride (0.8 M in diglyme) through the setup according to Scheme 6.15 using a dual syringe pump. At each flow rate, the system was stabilised for three residence times and then integrals of TMSCF₂H were measured in comparison to the trifluorotoluene standard for one residence time. Each spectrum was acquired using only one scan and the frequency of spectra acquisition adjusted depending on the flow rate. For fast flow rates the frequency was high (highest frequency possible approximately every 7 s) and for flow rates the frequency was lower (e.g. 0.66 mL/min flow rate, 30 min residence time, 2 min frequency of spectra acquired). The acquired spectra were integrated using the InsightMR software, the data exported into Excel and converted into a graph showing the integration over time. The yields were calculated from the integral of the trifluorotoluene standard and the integral of the compound after stabilisation (after 3 residence times), averaged and the standard error in the mean calculated, which proved to be a maximum of 0.3% for all measurements. Applying this method for all residence times/ flow rates gave the TMSCF₂H yield for different residence times resulting from the change in flow rates.

4.4. Telescoped large scale synthesis of TMSCF₂H

Solutions of sodium borohydride (0.8 M) and trifluoromethyltrimethylsilane (2.4 M) in diglyme were prepared and pumped through the flow system using HPLC pumps at 2 mL/min each (residence time 30 s, see Supporting Information). After 1 minute (allowing the system to reach steady state), the output was fed directly into a flask and stirred at 50 °C.

After 75 minutes (51 g, 360 mmol starting material processed), the pumps were stopped and the flask stirred at 50 °C for another 30 minutes. The temperature was increased to 180 °C and crude product collected by distillation. Further distillation (b.p. 65 - 70 °C) yielded difluoromethyltrimethylsilane (25.04 g, 202 mmol, 56%) as a colourless liquid.

¹H NMR (400 MHz, CDCl₃) δ 5.85 (t, *J* = 46.2 Hz, 1H), 0.17 (s, 9H, CH₃) ppm.

¹⁹F NMR (376 MHz, CDCl₃) δ -139.54 (d, *J* = 46.3 Hz, 2F) ppm.

¹³C NMR (101 MHz, CDCl₃) δ 124.0 (t, *J* = 254.1 Hz, CF₂H), -5.0 (CH₃) ppm.

IR: 2963, 2903, 1321, 1256, 1078, 989, 858 cm⁻¹. Data is consistent with literature reports.²ⁿ

Acknowledgments

D.L.B. and R.J. thank the School of Chemistry at Cardiff University for generous support and a studentship to C.S. Cambridge Reactor Design are thanked for a studentship (J.L.H.). Martin Hofmann and Peter Gierth from Bruker are thanked for useful discussions and technical support.

References and notes

1. a) J. L. Howard, W. Nicholson, Y. Sagatov and D. L. Browne, *Beilstein J. Org. Chem.*, 2017, **13**, 1950-1956; b) C. N. Neumann and T. Ritter, *Angew. Chem. Int. Ed.*, 2015, **54**, 3216-3221. c) D. L. Browne and P. Richardson, in *Synthetic Methods in Drug Discovery: Volume 2*, 2016, pp. 263-370. d) M. Baumann, I. R. Baxendale, L. J. Martin and S. V. Ley, *Tetrahedron*, 2009, **65**, 6611-6625. e) T. Liang, C. N. Neumann and T. Ritter, *Angew. Chem. Int. Ed.*, 2013, **52**, 8214-8264. f) B. E. Smart, *J. Fluor. Chem.*, 2001, **109**, 3-11. g) R. Filler and R. Saha, *Future Med. Chem.*, 2009, **1**, 777-791. h) W. K. Hagmann, *J. Med. Chem.*, 2008, **51**, 4359-69.
2. a) T. Hu, I. Baxendale and M. Baumann, *Molecules*, 2016, **21**, 918; b) D. Chen, C. Ni, Y. Zhao, X. Cai, X. Li, P. Xiao and J. Hu, *Angew. Chem. Int. Ed.*, 2016, **55**, 12632-12636; c) Y. Zhao, W. Huang, J. Zheng and J. Hu, *Org. Lett.*, 2011, **13**, 5342-5345; d) A. A. Tyutyunov, V. E. Boyko and S. M. Igoumnov, *Fluorine notes*, 2011, **1**, 78; e) P. S. Fier and J. F. Hartwig, *J. Am. Chem. Soc.*, 2012, **134**, 5524-5527; f) X.-L. Jiang, Z.-H. Chen, X.-H. Xu and F.-L. Qing, *Organic Chemistry Frontiers*, 2014, **1**, 774-776; g) Y. Gu, X. Leng and Q. Shen, *Nat. Commun.*, 2014, **5**; h) C. Matheis, K. Jouvin and L. J. Goossen, *Org. Lett.*, 2014, **16**, 5984-5987; i) G.-F. Du, Y. Wang, C.-Z. Gu, B. Dai and L. He, *RSC Advances*, 2015, **5**, 35421-35424; j) D. Zhu, Y. Gu, L. Lu and Q. Shen, *J. Am. Chem. Soc.*, 2015, **137**, 10547-10553; k) S.-Q. Zhu, X.-H. Xu and F.-L. Qing, *Organic Chemistry Frontiers*, 2015, **2**, 1022-1025; l) K. Jouvin, C. Matheis and L. J. Goossen, *Chemistry-A European Journal*, 2015, **21**, 14324-14327; m) J. Wu, Y. Gu, X. Leng and Q. Shen, *Angew. Chem. Int. Ed.*, 2015, **54**, 7648-7652; n) B. Bayarmagnai, C. Matheis, K. Jouvin and L. J. Goossen, *Angew. Chem. Int. Ed.*, 2015, **54**, 5753-5756; o) E. Obijalska, G. Utecht, M. K. Kowalski, G. Młostoń and M. Rachwalski, *Tetrahedron Lett.*, 2015, **56**, 4701-4703; p) O. M. Michurin, D. S. Radchenko and I. V. Komarov, *Tetrahedron*, 2016, **72**, 1351-1356; q) 2016; r) G. K. S. Prakash, S. K. Ganesh, J.-P. Jones, A. Kulkarni, K. Masood, J. K. Swaback and G. A. Olah, *Angew. Chem. Int. Ed.*, 2012, **51**, 12090-12094; s) Q. Glenadel, E. Ismalaj and T. Billard, *J. Org. Chem.*, 2016, **81**, 8268-8275; t) L. Wang, J. Wei, R. Wu, G. Cheng, X. Li, J. Hu, Y. Hu and R. Sheng, *Organic Chemistry Frontiers*, 2017, **4**, 214-223; u) J. Xu, S. Zhang, S. Wu, S. Bi, X. Li, Y. Lu and L. Wang, *Tetrahedron*, 2017, **73**, 494-499; v) J. R. Bour, S. K. Kariofillis and M. S. Sanford, *Organometallics*, 2017, **36**, 1220-1223; w) C. Lu, Y. Gu, J. Wu, Y. Gu and Q. Shen, *Chem. Sci.*, 2017, **8**, 4848-4852; x) C. D. Sessler, M. Rahm, S. Becker, J. M. Goldberg, F. Wang and S. J. Lippard, *J. Am. Chem. Soc.*, 2017, **139**, 9325-9332; y) E. Pietrasiak and A. Togni, *Organometallics*, 2017, **36**, 3750-3757; z) S.-Q. Zhu, X.-H. Xu and F.-L. Qing, *Chem. Commun.*, 2017, **53**, 11484-11487.
3. a) J. L. Howard, C. Schotten, S. T. Alston and D. L. Browne, *Chem. Commun.*, 2016, **52**, 8448-8451; b) J.-B. Han, H.-L. Qin, S.-H. Ye, L. Zhu and C.-P. Zhang, *J. Org. Chem.*, 2016, **81**, 2506-2512.
4. a) A. Tyutyunov, V. Boyko and S. Igoumnov, *Fluorine notes*, 2011, **1**, 74. For a comprehensive overview of safety assessment in the development and operation of modular continuous-flow processes see: b) N. Kockmann, P. Thenée, C. Fleischer-Trebes, G. Laudadio and T. Noël, *React. Chem. Eng.*, 2017, **2**, 258-280.
5. M. Movsisyan, E. I. P. Delbeke, J. K. E. T. Berton, C. Battilocchio, S. V. Ley and C. V. Stevens, *Chem. Soc. Rev.*, 2016, **45**, 4892-4928.
6. a) J. L. Howard, C. Schotten and D. L. Browne, *React. Chem. Eng.*, 2017, **2**, 281-287; b) D. L. Browne, J. L. Howard and C. Schotten, in *Comprehensive Medicinal Chemistry III*, Elsevier, Oxford, 2017, DOI: <https://doi.org/10.1016/B978-0-12-409547-2.12288-7>, pp. 135-185; c) J. C. Pastre, D. L. Browne and S. V. Ley, *Chem. Soc. Rev.*, 2013, **42**, 8849-8869; d) J. Wegner, S. Ceylan and A. Kirschning, *Adv. Synth. Catal.*, 2012, **354**, 17-57; e) T. Wirth, *ChemSusChem*, 2012, **5**, 215-216; f) S. Born, E. O'Neal and K. F. Jensen, in *Comprehensive Organic Synthesis II, Volume 9: Enabling Technologies for Organic Synthesis*, eds. P. Knochel and G. A. Molander, Elsevier, Amsterdam, 2014, DOI: <https://doi.org/10.1016/B978-0-08-097742-3.00912-5>, pp. 54-93; g) M. B. Plutschack, B. Pieber, K. Gilmore and P. H. Seeberger, *Chem. Rev.*, 2017, **117**, 11796-11893; h) T. Noël, Y. Su and V. Hessel, in *Organometallic Flow Chemistry*, ed. T. Noël, Springer International Publishing, Cham, 2016, DOI: 10.1007/3418_2015_152, pp. 1-41; i) D. T. McQuade and P. H. Seeberger, *J. Org. Chem.*, 2013, **78**, 6384-6389; j) B. Gutmann, D. Cantillo and C. O. Kappe, *Angew. Chem. Int. Ed.*, 2015, **54**, 6688-6728; k) D. Dallinger and C. O. Kappe, *Current Opinion in Green and Sustainable Chemistry*, 2017, **7**, 6-12; l) J. Britton and T. F. Jamison, *Nat. Protoc.*, 2017, **12**, 2423; m) D. Webb and T. F. Jamison, *Chem. Sci.*, 2010, **1**, 675-680; n) R. Porta, M. Benaglia and A. Puglisi, *Org. Process Res. Dev.*, 2015, **20**, 2-25; o) M. Baumann and I. R. Baxendale, *Beilstein J. Org. Chem.*, 2015, **11**, 1194-1219; p) T. Wirth, *Microreactors in organic chemistry and catalysis*, John Wiley & Sons, 2013.
7. a) D. L. Browne, S. Wright, B. J. Deadman, S. Dunnage, I. R. Baxendale, R. M. Turner and S. V. Ley, *Rapid Commun. Mass Spectrom.*, 2012, **26**, 1999-2010; b) D. C. Fabry, E. Sugiono and M. Rueping, *Isr. J. Chem.*, 2014, **54**, 341-350; c) D. C. Fabry, E. Sugiono and M. Rueping, *React. Chem. Eng.*, 2016, **1**, 129-133; d) F. Zhao, D. Cambié, V. Hessel, M. G. Debijs and T. Noël, *Green Chem.* 2018, DOI:10.1039/c8GC00613J.
8. a) T. Brodmann, P. Koos, A. Metzger, P. Knochel and S. V. Ley, *Org. Process Res. Dev.*, 2012, **16**, 1102-1113; b) N. Holmes, G. R. Akien, A. J. Blacker, R. L. Woodward, R. E. Meadows and R. A. Bourne, *React. Chem. Eng.*, 2016, **1**, 366-371; c) N. Holmes, G. R. Akien, R. J. D. Savage, C. Stanetty, I. R. Baxendale, A. J. Blacker, B. A. Taylor, R. L. Woodward, R. E. Meadows and R. A. Bourne, *React. Chem. Eng.*, 2016, **1**, 96-100; d) M. O'Brien, L. Konings, M. Martin and J. Heap, *Tetrahedron Lett.*, 2017, **58**, 2409-2413; e) K. Gilmore, D. Kopetzki, J. W. Lee, Z. Horváth, D. T. McQuade, A. Seidel-Morgenstern and P. H. Seeberger, *Chem. Commun.*, 2014, **50**, 12652-12655; f) D. E. Fitzpatrick, C. Battilocchio and S. V. Ley, *Org. Process Res. Dev.*, 2016, **20**, 386-394; g) S. V. Ley, D. E. Fitzpatrick, R. J. Ingham and R. M. Myers, *Angew. Chem. Int. Ed.*, 2015, **54**, 3449-3464; h) S. V. Ley, D. E. Fitzpatrick, R. M. Myers, C. Battilocchio and R. J. Ingham, *Angew. Chem. Int. Ed.*, 2015, **54**, 10122-10136; i) M. I. Jeraal, N. Holmes, G. R. Akien and R. A. Bourne, *Tetrahedron*, 2018, DOI: <https://doi.org/10.1016/j.tet.2018.02.061>; j) R. A. Skilton, A. J. Parrott, M. W. George, M. Poliakoff and R. A. Bourne, *Appl. Spectrosc.*, 2013, **67**, 1127-1131; k) A. J. Parrott, R. A. Bourne, G. R. Akien, D. J. Irvine and M. Poliakoff, *Angew. Chem. Int. Ed.*, 2011, **50**, 3788-3792. l) V. Dragone, V. Sans, A. B. Henson, J. M. Granda and L. Cronin, *Nat. Commun.*, 2017, **8**, 15733. m) V. Sans, L. Porwol, V. Dragone and L. Cronin, *Chem. Sci.*, 2015, **6**, 1258-1264; n) V. Sans and L. Cronin, *Chem. Soc. Rev.*, 2016, **45**, 2032-2043.
9. a) M. V. Gomez and A. de la Hoz, *Beilstein J. Org. Chem.*, 2017, **13**, 285; b) K. Albert, *On-line LC-NMR and related techniques*, John Wiley & Sons, 2003; c) K. Albert and E. Bayer, *TrAC Trends in Analytical Chemistry*, 1988, **7**, 288-293; d) M. Maiwald, H. H. Fischer, Y.-K. Kim, K. Albert and H. Hasse, *J. Magn.*

- Reson.*, 2004, **166**, 135-146; e) S. S. Zalesskiy, E. Danieli, B. Blümich and V. P. Ananikov, *Chem. Rev.*, 2014, **114**, 5641-5694; f) N. Zientek, K. Meyer, S. Kern and M. Maiwald, *Chem. Ing. Tech.*, 2016, **88**, 698-709; g) M. Goldbach, E. Danieli, J. Perlo, B. Kaptein, V. M. Litvinov, B. Blümich, F. Casanova and A. L. L. Duchateau, *Tetrahedron Lett.*, 2016, **57**, 122-125; h) M. A. Vargas, M. Cudaj, K. Hailu, K. Sachsenheimer and G. Guthausen, *Macromolecules*, 2010, **43**, 5561-5568; i) V. Röntzsch, M. Wilhelm and G. Guthausen, *Magn. Reson. Chem.*, 2016, **54**, 494-501; j) M. A. Bernstein, M. Štefinović and C. J. Sleight, *Magn. Reson. Chem.*, 2007, **45**, 564-571; k) A. Nordon, C. A. McGill and D. Littlejohn, *Analyst*, 2001, **126**, 260-272; l) M. V. Silva Elipse and R. R. Milburn, *Magn. Reson. Chem.*, 2016, **54**, 437-443; m) B. Picard, B. Gouilleux, T. Lebleu, J. Maddaluno, I. Chataigner, M. Penhoat, F.-X. Felpin, P. Giraudeau and J. Legros, *Angew. Chem. Int. Ed.*, 2017, **56**, 7568-7572; n) D. A. Foley, C. W. Doecke, J. Y. Buser, J. M. Merritt, L. Murphy, M. Kissane, S. G. Collins, A. R. Maguire and A. Kaerner, *J. Org. Chem.*, 2011, **76**, 9630-9640; o) B. Ahmed-Omer, E. Sliwinski, J. P. Cerroto and S. V. Ley, *Org. Process Res. Dev.*, 2016, **20**, 1603-1614; p) C. A. Fyfe, M. Cocivera and S. W. H. Damji, *Acc. Chem. Res.*, 1978, **11**, 277-282; q) J. Y. Buser and A. D. McFarland, *Chem. Commun.*, 2014, **50**, 4234-4237; r) J. Bart, A. J. Kolkman, A. J. Oosthoek-de Vries, K. Koch, P. J. Nieuwland, H. Janssen, J. van Bentum, K. A. M. Ampt, F. P. J. T. Rutjes, S. S. Wijmenga, H. Gardeniers and A. P. M. Kentgens, *J. Am. Chem. Soc.*, 2009, **131**, 5014-5015; s) G. Finch, A. Yilmaz and M. Utz, *J. Magn. Reson.*, 2016, **262**, 73-80. t) A. M. R. Hall, J. C. Chouler, A. Codina, P. T. Gierth, J. P. Lowe and U. Hintermair, *Catal. Sci. Technol.*, 2016, **6**, 8406-8417. u) B. Musio, E. Gala and S. V. Ley *ACS Sustainable Chem. Eng.* 2018, **6**, 1489-1495.
10. a) M. Khajeh, M. A. Bernstein and G. A. Morris, *Magn. Reson. Chem.*, 2010, **48**, 516-522; b) D. A. Foley, E. Bez, A. Codina, K. L. Colson, M. Fey, R. Krull, D. Piroli, M. T. Zell and B. L. Marquez, *Anal. Chem.*, 2014, **86**, 12008-12013; c) A. M. R. Hall, J. C. Chouler, A. Codina, P. T. Gierth, J. P. Lowe and U. Hintermair, *Catal. Sci. Tech.*, 2016, **6**, 8406-8417; d) D. A. Foley, A. L. Dunn and M. T. Zell, *Magn. Reson. Chem.*, 2016, **54**, 451-456; e) D. A. Foley, J. Wang, B. Maranzano, M. T. Zell, B. L. Marquez, Y. Xiang and G. L. Reid, *Anal. Chem.*, 2013, **85**, 8928-8932; f) A. M. R. Hall, R. Broomfield-Tagg, M. Camilleri, D. R. Carbery, A. Codina, D. T. E. Whittaker, S. Coombes, J. P. Lowe and U. Hintermair, *Chem. Commun.*, 2018, **54**, 30-33.

Supplementary Material

Supplementary material that may be helpful in the review process should be prepared and provided as a separate electronic file. That file can then be transformed into PDF format and submitted along with the manuscript and graphic files to the appropriate editorial office.